ELSEVIER

Coordination Chemistry Reviews
190–192 (1999) 209–229

COORDINATION CHEMISTRY REVIEWS

www.elsevier.com/locate/ccr

High-frequency EPR of transition ion complexes and metalloproteins

Wilfred R. Hagen *

Department of Molecular Spectroscopy, University of Nijmegen, Toernooiveld 1, 6525 ED Nijmegen, The Netherlands

Accepted 17 February 1999

Contents

Abstract

For more than 50 years EPR spectoscopists have worked predominantly with the standard X-band microwave frequency of 9–10 GHz. Technical developments now make it possible to do experiments on randomly-orientated samples using much higher microwave frequencies

* Tel.: +31-243-652260; fax: +31-243-652082.
E-mail address: hagen@sci.kun.nl (W.R. Hagen)

PII: S0010-8545(99)00079-X

and corresponding magnetic fields. For transition ion complexes this can not only result in drastically increased spectral resolution, but it also allows for the spectroscopy of high-spin systems that are undetectable in X-band due to large zero-field interactions. In practice these new possibilities are limited by a concentration sensitivity that decreases with increasing microwave frequency.

Keywords: EPR; ESR; High frequency; High field; High spin; Metalloprotein

1. Introduction

This review surveys the recent developments in high-frequency/high-field electron paramagnetic resonance spectroscopy with emphasis on applications to molecular coordination complexes in particular metalloproteins and their models. High frequency is operationally defined as 'significantly higher than Q-band (35 GHz)'; similarly, high field is defined as 'beyond the limits of conventional electromagnets'. Typical values employed at present are 75–400 GHz and 3–15 T. The major goal of this review is to provide chemists with sufficient background information to allow them to evaluate the potential usefulness of hf-EPR for their own work and to make an educated guess on the sample requirements. The physics of the recent developments in hardware will only be outlined in brief in so far as this is required for a basic understanding of the experiment. The review is limited to molecular transition complexes including molecular clusters; organic radicals are excluded from consideration and so are systems with long-range cooperative interactions.

2. Concepts

2.1. What is high-frequency EPR

Not long after Zavoisky discovered the EPR effect Bagguley and Griffiths, 1947 pushed the frequency of the microwave, used to induce the magnetic dipole transitions, up into the X-band 9–10 GHz [1], and this has been the dominant frequency in EPR spectroscopy over the last five decades. X-band EPR is likely to remain the standard for some time to come. Occasionally (i.e. in less than 10% of all studies) other frequencies have been employed, notably Q-band ($\sim$ 35 GHz) which has been available commercially from Varian Inc, USA, in the 1960s. Lower frequencies, S-band ($\sim$ 3 GHz) and L-band ($\sim$ 1 GHz), became available commercially in the early 1980s from Bruker AG in Germany. Most of these spectrometers have two things in common: they use a resonant structure, or cavity, operated at its fundamental mode. This means that the cavity has the dimension of the wavelength of the microwave. Also, the required magnetic fields corresponding to $g_e = 2$ can be made using conventional electromagnets (i.e. ≤ 3 T). The first commercial high-frequency (95 GHz) spectrometer was recently marketed [2]. Typical frequency bands used in EPR spectroscopy and their related field values are given in Table 1.

It is clear from Table 1 that the use of frequencies above the E-band implies that the electromagnet should be replaced with a different type and that the use of frequencies above ca. 0.5 THz requires magnets that are only available in a few highly specialized laboratories. Also, from the column with wavelength values it can be seen that conventional 'single-mode' resonators will become exceedingly difficult to construct and to operate at frequencies approximately above D-band.

In short, a high-frequency EPR spectrometer differs from the standard X-band machine typically in terms of a different type of microwave source, a different type of resonator, and a different type of magnet.

2.2. Why should one do high-frequency EPR

Fig. 1 illustrates the usefulness of high-frequency EPR by comparing hf data to equivalent X-band data on a normalized scale (i.e. a $1/g$ scale). The traces are simulated spectra; the original, non-normalized data can be found in [3].

In X-band the $S = 1/2$ system Cr(V) in $Na_3Cr(O_2)_4$ gives a single, broad, virtually structureless line; however, at 375 GHz the same compound gives a well resolved rhombic spectrum whose three g-values can be interpreted in terms of symmetry and electronic properties [3]. A second example: in X-band the $S = 2$ system Mn(III) in the tetrapyrrole system Mn(TPP)Cl gives no spectrum at all, while at 226 GHz a well defined transition is observed [4]. A third example: in X-band at ambient temperature the $S = 7/2$ system Gd(III) in water gives a single line of 67

Table 1
EPR microwave frequency bands with associated wavelengths, energies, and magnetic fields for $g = 2$

Band	Typical frequency ν (GHz)	Wavelength λ (mm)	Energy E (cm^{-1})	Field B at $g = 2$ (T)
L-band	1	300	0.03	0.03
S-band	3	100	0.1	0.11
C-band	4	75	0.13	0.14
X-band	**9**	**33**	**0.3**	**0.32**
P-band	15	20	0.5	0.54
K-band	24	12.5	0.8	0.86
Q-band	35	8.5	1.2	1.25
U-band	50	6.0	1.7	1.8
V-band	65	4.6	2.2	2.3
E-band	75	4	2.5	2.7
W-band	95	3	3.2	3.4
F-band	110	2.7	3.7	3.9
D-band	130	2.3	4.3	4.6
(Unnamed)	190	1.6	6.3	6.8
(Unnamed)	285	1	9.5	10.2
(Unnamed)	380	0.79	12.7	13.6
(Unnamed)	475	0.63	15.8	17
(Unnamed)	570	0.52	19	20.4
(Unnamed)	1000	0.3	33.4	35.7

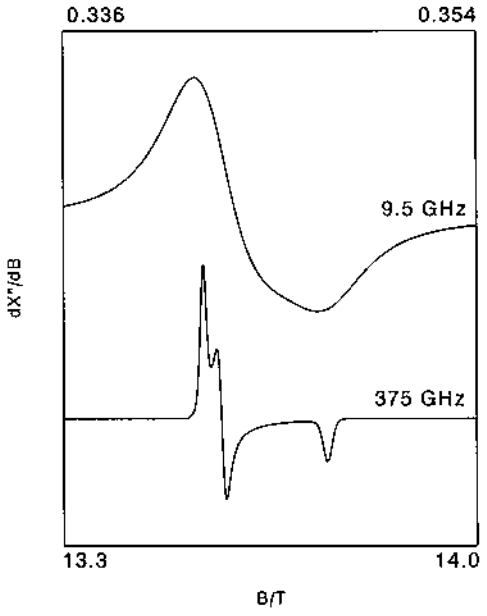

Fig. 1. A comparison of normalized EPR spectra at 9.5 versus 375 GHz of the $3d^1$ $S = 1/2$ system Cr(V) in pure, undiluted $Na_3Cr(O_2)_4$ to illustrate dramatic resolution enhancement at high frequency.

mT width; at 140 GHz the line is only 4.5 mT and its temperature dependence is related to the relaxation time T_1 [5,6]. These examples illustrate the major reasons for using high-frequency EPR: for some systems the spectral resolution increases, other systems turn from 'EPR-silent' to 'EPR-detectable', and for yet other systems the study of a specific interaction (e.g. relaxation) becomes tractable.

Table 2
Spectroscopic subjects in hf-EPR

Resolution enhancement
g-matrix resolved from hyperfine tensor
g-matrix resolved from superhyperfine splittings
g-matrix resolved from exchange broadening
Improved orientation selection in ENDOR/ESEEM
Impossible systems
Integer-spin systems with large zfs ('EPR-silent' systems)
Half integer spin systems with large zfs (multiple transitions)
Small crystals (high filling factors)
Novel subjects
Double-quantum transitions
D-strain (inhomogeneous broadening)
Spin-lattice relaxation at high frequencies
Higher-power terms in B in the spin-Hamiltonian

Table 2 enumerates possible subjects of research from the point of view of the spectroscopist, i.e. without reference to a specific chemical system. Examples of applications will be given in the section. The theoretical principles underlying most of these phenomena are simple and straightforward, although the numerical analysis in specific cases may well be quite involved. The electronic structure of a compound defines its paramagnetism, and a detailed analysis of the latter provides an in-dept study of the former. The paramagnetism is traditionally described in the frame of the spin Hamiltonian, $\boldsymbol{H}$. This formalism is an effective description of the magnetic ground state in terms of interactions between three types of entities: B, S, I, magnetic field(s), electron spin(s), and nuclear spin(s). B is a vector, S and I are vector operators. The dominant interactions are the five bilinear ones: $B \times S$, $S \times S$, $B \times I$, $S \times I$, and $I \times I$, i.e. the Zeeman, zero-field, nuclear Zeeman, hyperfine, and quadrupolar interactions. In the spin Hamiltonian these are written as vector–matrix–vector inproducts where the components of the coupling matrix are the measurable parameters. For example, the electronic Zeeman interaction is written as $\beta B \cdot g \cdot S$, where β, the Bohr magneton, is a normalization constant, and the elements of the **g**-matrix (the 'g-values') are the measurable parameters.

The crux of high-frequency EPR (or of EPR at variable frequency in general) is the fact that of all interactions determining the paramagnetism, and therefore the EPR spectrum, some are dependent on the external magnetic field B (typically linearly dependent) while others are independent of B:$\boldsymbol{H} = \Sigma C_{\mathrm{B}}(B) + \Sigma C_0$. Increasing the microwave frequency, and therefore increasing the external magnetic field, will make the interactions with coefficients C_{B} more important than the interactions with C_0.

It should be noted that although there are only five bilinear combinations of B, S, and I (two of which, nuclear Zeeman and quadrupolar interactions, may only be significant in ENDOR or ESEEM spectroscopy) the actual number of interactions contributing to the spectra is not necessarily a small number. The electron spin, S, can be related to a single electron (low spin) or to multiple electrons (high spin) on a single nucleus, but it can also be related to the system spin of a cluster (exchange interactions), or to different intra- or intermolecular sites (dipolar interactions). Similarly, the nuclear spin, I, can be related to the central nucleus, to coordinating ligands, to higher coordination sphere ligands. Furthermore, each interaction can be distributed reflecting a distribution in structure or conformation: g-strain (distributed Zeeman interaction), D-strain (distributed zero-field interaction), etc. These distributed quantities define the shape and width of the inhomogeneously broadened resonance line.

However, the number of B-dependent interactions is usually small. In continuous-wave EPR the only static B-dependent terms are the electronic Zeeman interaction and its distribution, g-strain [7]. High-frequency EPR essentially means to increase the importance of these two interactions at the expense of all other interactions. It should be realized that this game can work out two ways: firstly, when at X-band a B-independent interaction is less strong than the electronic Zeeman interaction (cf. a hyperfine interaction, or, in a metalloprotein, an intramolecular dipolar interaction) then increasing the frequency will result in its

reduction and ultimate disappearance from the EPR spectrum. This typically leads to a simplification of the spectrum. On the other hand, when a B-independent interaction dominates the X-band spectrum (e.g. the zero-field interaction in many high-spin transition complexes) then the spectrum is relatively insensitive to frequency variation (and relatively uninformative from a chemist's point of view), and is readily described, using the well known rhombograms in terms of effective g-values [8]. Here, a drastic increase in microwave frequency will lead to a more complex EPR spectrum, but this will also be more informative chemically. In these high-frequency spectra an added complexity comes from the fact that, since the effect of the zero-field interaction now rapidly varies with frequency, its distribution (D-strain) does also and therefore contributes significantly to the shape and width of the resonance line.

3. Practical considerations

3.1. Where to go to for high-frequency EPR

This question is dictated by the choice on what type of spectrometer is suitable for a specific experiment. A high-frequency EPR spectrometer may differ from a standard EPR spectrometer in one, more, or all of its basic components. However, each of these components comes in several drastically different varieties. All permutations are in principle possible and many of these are, at the present time, in the course of being evaluated for usefulness in chemical applications.

The six basic components of an EPR spectrometer (cf. [9]) are: a source of microwaves, a system to transfer microwaves, a resonator (containing the sample), a detector of reflected (or transmitted) microwaves, a scanning magnet, and a system to control the sample temperature. In Table 3 each of these components is subdivided. The first sub-entry is the component of a typical standard X-band machine, and subsequent sub-entries are approximately given in increasing order of 'unusualness'.

The traditional source of EPR microwaves, the klystron, is a narrow-band vacuum-tube device with a typical output of 10^{-1} W. Even in X-band spectrometers the klystron is nowadays usually replaced with the Gunn diode, a solid-state device of similar specifications. Practical Gunn diodes are available up to ca. 100 GHz. In hf-EPR spectrometers Gunn diode sources are frequently multiplied, using devices called doublers, triplers, etc., to obtain a multiple of the basic frequency at a reduced output power [10,11]. As an example, the 'unnamed' frequencies in Table 1 are multiples of a 95 GHz W-band source. Multiplication to very high frequencies, ≥ 0.5 THz, results in unworkably low powers. In this range the only practical sources available are far-IR lasers [12–15]; there is virtually no limit to the frequency, but the typical power is relatively low. In the intermediate range of a few hundred GHz alternative sources are available which may however have specific disadvantages: carcinotrons [16] (limited lifetime) and gyrotrons [17] (expensive: require their own superconducting magnet).

Table 3
Components for hf-EPR spectrometers

Sources	Klystrons
	Gunn diodes
	Avalanche diodes (IMPATTs)
	Multiplied Gunn diodes
	Backward-wave oscillators/carcinotrons
	FIR lasers
	Gyrotrons
Guides	Cutoff waveguide
	Oversized waveguide
	Horns
	Free space
Resonators	Fundamental-mode cavities
	Oversized cavities
	Fabry–Pérot resonators
	Whispering gallery mode resonators
	None (transmission or reflection)
Detectors	Diodes
	InSb bolometers
	Harmonic mixers
Magnets	Electromagnets
	Superconducting
	Bitter-type resistive
	Hybrids
Inserts	Cryogenic
	High-temperature
	Reversed cryostats

In a standard spectrometer microwaves ($\lambda \approx 3$ cm) are transported with low losses through rectangular waveguides 'at cutoff' (i.e. with cross-dimensions $\lambda^*\lambda/2$). At lower frequencies coaxials can be used. With increasing frequency waveguides become more lossy: spurious standing waves build up more readily on mechanical imperfections. A hf-spectrometer commonly uses rectangular or cylindrical oversized waveguides (i.e. with dimensions $\gg \lambda$) at least for part of its transport system [18,19]. This construction also implies the use of dimensional adaptors or tapers. The ultimate oversized waveguide is of course free space, and the associated tapers are called horns. The properties of mm waves and sub-mm waves in free space or in highly oversized waveguides are indicated as Gaussian-beam behavior (cf. [20]), and the set of devices used to modify them are collectively indicated with the term 'quasi optics'. The quasi means that devices are equivalent to those used in classical optics, however, they are not usually transparent to visible light: e.g. high-density polyethylene lenses [19], gold-film mirrors [21].

Matching the cutoff waveguide in a standard spectrometer the resonator (or: cavity, probehead) is of the fundamental-mode type: it is highly optimized for a lower-limit frequency with wavelength, λ, equal to a dimension of the resonator. Cylindrical fundamental-mode resonators are practical up to ca. 150 GHz [22–24]. At increasing frequencies one can employ overtones in oversized cavities [25]. Or

one can use a mm-wave bridge in combination with open, quasi-optical resonators, e.g. Fabry–Pérot resonators [19,21,26–30]. The ultimate extrapolation of the latter is to use no resonator at all [12,16,18], which is a common choice in hf-spectrometers using fir laser sources. This results in a conceptually, and constructionally simple structure for straightforward EPR transmission or reflection experiments, however, with low intrinsic sensitivity. Novel devices are also explored such as the whispering gallery mode resonator [31,32], a disc-like structure with a circumference that is a multiple, n, of the wavelength of the microwave. Typically, $n = 50–100$ resulting in coin-sized discs for hf-EPR. The sample is placed on the rim of the disc.

The primary detector of X-band microwaves is a simple and cheap diode. Diodes become increasingly noisy at higher frequencies. Detectors in hf-EPR spectrometers are typically more complex and costly. InSb bolometers [12,24] are cooled with liquid He. A heterodyne detection system built around a harmonic mixer requires two independent microwave sources, an excitation source and a detector local oscillator; the former is hf, the latter may be a few GHz [33] or hf [24,34].

A major cost item in a hf-EPR spectrometer is the magnet. Electromagnets are used in standard spectrometers but these are limited to fields < 3 T. From W-band onwards superconducting magnets are required to obtain fields equivalent to $g_e = 2$ (cf. Table 1). For spectra of limited field range (radicals) it may suffice to operate a supercon in persistent mode combined with a sweeping coil [35]. However, many applications in transition metal chemistry, particularly hf-EPR of high-spin systems, will require a fully scannable magnet from zero to maximum field. Resistive magnets of the Bitter type [36] then become a practical alternative for supercons, especially when the demands on field homogeneity and reproducibility are not as high as for narrow radical spectra. Resistive magnets require huge electric power supplies, typically producing 10^7 W, therefore they are only available in specialized laboratories. For high fields, > 20 T, no superconducting magnets are available, and the resistive magnet becomes the only alternative. Higher fields, > 30 T, can be produced with hybrid magnets which are concentrical combinations of a resistive magnet inside a superconducting magnet. Even higher fields, > 40 T, can be made with pulsed magnets but their use would require a major adaptation of the spectrometer. This possibility has not been explored yet for hf-EPR. Note that the quoted field limits are indicative only; they increase constantly as magnet technology progresses.

In standard spectrometers the sample can usually be cooled, to 4.2 K or lower, or heated, to 100°C or higher. Also, single-crystal samples can be oriented, and rf coils may be available for double resonance. To add these provisions to a hf spectrometer is not trivial because of the limited space available e.g. as determined by the bore of the magnet. Even a measurement of a sample at room temperature (r.t.) may require special equipment (a reversed cryostat) in systems with a bore cooled permanently by the magnet's own cryogenics.

3.2. How to plan a high-frequency experiment

It should be clear from the above that a hf-EPR experiment in coordination chemistry requires careful planning in terms of sufficient conditions regarding

frequency, field, temperature, and sensitivity. Perhaps the following crude division into three types of spectrometers derived from field/frequency ranges is useful as an initial orientation. (I) Classical spectrometers: up to 3 T/75 GHz the complete spectrometer can be made of standard components. Sensitivity is usually high. (II) hf-Spectrometers: up to some 15 T/0.5 THz the spectrometer is likely to use a Fabry–Pérot resonator and related quasi-optical devices. The magnet may be a supercon or a resistive one. Sensitivity is lowered. (III) Very-hf-spectrometers: above 0.5 THz the spectrometer is likely to be based on transmission of waves from an fir laser. The magnet will probably be resistive. The sensitivity will be low.

Some readers may find the given qualitative indications of sensitivity to be counter-intuitive (or even at contrast with some claims from the field). Should not sensitivity increase with frequency as in NMR spectroscopy? The simple answer is that *absolute* sensitivity probably increases with frequency if the microwave part of the spectrometers is made according to a single concept. For example, less milligrams of a dilute material with $S = 1/2$ may be required to reach the detection limit of a single-mode resonator at 100 GHz than for an equivalent one at 10 GHz. The volume of the 100 GHz resonator is 10^3 times less than that of the 10 GHz resonator, therefore, the 'filling factor' is much more favorable when sample is limited. In practice, however, this is a relatively rare situation (the exception is: small single crystals, especially of metalloproteins) because the maximal amount of sample for a single-mode 100 GHz resonator is of the order of 1 mg! If 1 g is available, then the X-band spectrometer will almost certainly produce a better S/N ratio. One of the major reasons for limited sensitivity at high frequency (and, unfortunately, not yet documented in a quantitative manner in the literature) is probably the increased ease with which unwanted passage effects (resulting in unwanted spectral deformations such as partial integration) occur in hf-EPR. Theorization on this subject is in its infancy as virtually no data are available as yet on paramagnetic relaxation at high frequencies.

The advised practical approach for the coordination chemist when contacting the hf-EPR spectroscopist is to rebut any claim on absolute sensitivity with an inquiry on *concentration* sensitivity preferably documented on a sample comparable to the prospective object of study. This information is even more important for the bioinorganic chemist as many biological systems of interest cannot be prepared in concentrations above ca. 1 mM. While much research effort still goes into sensitivity improvement, at this time 1 mM may actually be the detection limit for broader spectra in certain hf-EPR spectrometers. On the other hand, recall (cf. Fig. 1A) that pure, undiluted coordination complexes may be used as they give highly resolved hf-EPR spectra.

It is not a trivial matter to accurately measure the strength of a magnetic field of the order of 10 T at the position of the sample. Although hf-EPR may in principle allow for very accurate determinations of g-values, in many practical settings this goal may require measurements on internal and external field calibration standards (the six-line $I = 5/2$ pattern from Mn^{2+} in, e.g. MgO is a common marker) as well as measurements on field homogeneity and reproducibility.

A final point of concern is the limited thermal and/or chemical (e.g. redox) stability of certain samples especially biological ones. Spectrometer hardware developers use simple, stable test samples such as DPPH radical or Mn(II) in MgO. Once the spectrometer has been declared to be operational for outside use this does not necessarily include any facility to mount labile samples. Several hf spectrometers in their present status require loading in air at ambient temperature followed by slow cooling and anaerobiosis.

4. Applications

The hf-EPR studies described in the literature have been arranged below according to the chemical nature of the molecular system. A brief alternative arrangement according to the (system) spin of the ground state is presented in Table 4.

4.1. Mononuclear d-ion complexes

The spectrum of vanadium V(IV) ($3d^1$, $S = 1/2$, $I = 7/2$) from dilute frozen solutions of hydrated vanadyl ion (10 mM $VOSO_4$, 10 mM HCl, 2 M $NaClO_4$) was studied in D-band (130 GHz) and compared to X-band [24,37]. This axial system has $g_x = 1.97$, $g_z = 1.93$, $A_x = 7.4$ mT, $A_z = 19.9$ mT. In X-band this results in complete interference of the eight perpendicular hyperfine lines with the parallel hyperfine pattern. In D-band the two sets are fully separated. The inhomogeneous line width increases by a factor of ca. 5 while the frequency increases by $130/9 \approx 14$, therefore, the effective **g**-matrix resolution has increased. The D-band spectrum has absorption shape illustrating the difficulty in avoiding passage effects in hf-EPR especially when employing single-mode resonators.

Chromium Cr(V) ($3d^1$, $S = 1/2$, $I = 0$) has been studied in pure, undiluted salts of $M_3Cr(O_2)_4$ where $M_3 = Na_3$, K_3, or K_2Na [3]. This study illustrates the spectacular resolution enhancement that can be obtained in hf-EPR of pure compounds. In

Table 4
Spin systems studied by hf-EPR

Spin	System
$S = 1/2$	Cu^{2+}, VO^{2+}, Cr^{5+}
$S = 1$	Ni^{2+}, $(Cu^{2+})_8$
$S = 3/2$	$(Cu^{2+})_3$, Cr^{3+}
$S = 2$	Mn^{3+}
$S = 5/2$	Fe^{3+}, Mn^{2+}
$J = 7/2$	Gd^{3+}
$S = 9/2$	$(Mn^{3+;\,4+})_4$
$J = 6$	Tm^{3+}
$J = 15/2$	Er^{3+}
$S = 10$	Mn_{12}, $(Fe^{3+})_8$

X-band the spectra are severely broadened by exchange resulting in little or no resolution of the **g**-matrix. At a few hundred GHz exchange broadening has become insignificant and the remaining g-strain broadening is sufficiently small to allow for very well resolved g-values, e.g. $g = 1.9848, 1.9802, 1.9544$ for M = Na at 375 GHz (cf. Fig. 1). The nature of the broadening mechanisms requires further study and so does the question of the precise field dependence of the resolution enhancement.

Cr(II) high-spin ($3d^4$, $S = 2$) doped in ZnS, ZnSe, ZnTe has been measured from 30 to 210 GHz in fields up to 20 T [25,38]. This study illustrates nicely the strength of hf-EPR carried out at several frequencies for the analysis of integer-spin spectra with large zero-field splitting. In X-band the compounds are EPR silent ($|D| \gg hv$). With increasing frequency several transitions are sampled within the $S = 2$ manifold, allowing for accurate determination of D-values, -1.84 (ZnS), -2.48 (ZnSe) and $+2.29$ (ZnTe) cm^{-1}.

Iron Fe(III) high-spin ($3d^5$, $S = 5/2$) in tetrapyrrole systems typically has very strong zero-field interaction, $D \approx 10$ cm^{-1}, which makes these interesting subjects for hf- and very hf-EPR. In early work these determinations have been done with then available fir-sources on porphyrins [39,40] and dithiocarbamates [40]. There are no recent data except on proteins (see below).

High-spin $^{57}Fe(III)$ ($I = 1/2$) in a series of zeolites has been studied with W-band pulsed ENDOR [41]. At low temperature, 1.8 K, only the lowest EPR transition, $|-5/2>$ to $|-3/2>$, is observed. Furthermore, higher-order contributions to the hyperfine and zero-field interactions are insignificant at 95 GHz and this leads to simple spectra consisting of only two Fe ENDOR transitions at ca. 68 and 39 MHz. From these an isotropic hyperfine constant is determined, $a_0 \approx -29$ MHz, and this has been taken as evidence for the Fe to be in a zeolite framework T site.

Manganese Mn(II) high-spin ($3d^5$, $S = 5/2$, $I = 5/2$) in high symmetry hosts, typically has a very small zero-field interaction and insignificant g-anisotropy. The spectrum resulting from Mn(II) contaminant in MgO or Al_2O_3 is an essentially isotropic six-line pattern over a wide frequency range. It is therefore frequently used as a field and field-range marker in hf-EPR. Doped in $CaCO_3$ the Mn(II) spectrum has unusually narrow line width. As expected for an unresolved zero-field interaction from 85 to 179 GHz this line width is almost constant, from 3.5 to 4.1 Gauss [37], and this sample makes a good probe for field homogeneity.

Mn(III) high-spin ($3d^4$, $S = 2$) is an integer-spin system typically with $D \gg 0.3$ cm^{-1} and is therefore EPR silent in X-band. Mn(III) porphyrins have been studied in a spectrometer with the 113 GHz source multiplied to 226–452 GHz and with a fir source at 544 GHz [4]. For a pure, undiluted powder of Mn(TPP)Cl, TPP = tetraphenylporphyrinato, where $D = -2.27$ cm^{-1} and $g_{\|} = 1.822$, a signal from the $|-2>$ to $|-1>$ transition appears with 226 GHz close to zero field and its effective g-value decreases with increasing frequency. Contrary to previous bulk magnetic susceptibility experiments, four different Mn(III)porphyrins are clearly distinguishable on the basis of their D-value, and the results suggest the axial ligand (Cl vs. S) to be dominant in determining D.

Nickel Ni(II) high-spin ($3d^8$, $S = 1$) is a particularly interesting system at this stage of spectrometer development as it is well suited for the lower end of hf-EPR.

Zero-field spitting parameters are usually $D > 0.3$ cm^{-1}, typically $D \approx 1$ cm^{-1}. Some Ni(II) systems exhibit broad, incomplete spectra already in X-band; for others signals start to appear in Q-band. At frequencies of the order of 100 GHz the complete triplet spectrum should be detectable, and its overall features should be similar to the well known X-band triplet spectra from organic biradicals: two allowed anisotropic $\Delta m = 1$ transitions, a relatively isotropic half-field or $\Delta m = 2$ transition, and a very isotropic $\Delta m = 1 + 1$ double-quantum transition at full field. This has been verified in a study on Ni(II) doped $[Zn(en)_3](NO_3)_2$ which shows a broad feature at 9 GHz, a partly resolved, incomplete spectrum at 35 GHz, and a complete triplet pattern at 130 GHz with $g_{\|} = 2.181$, $g_{\perp} = 2.156$, $D = 0.832$ cm^{-1} [42] (see Fig. 2).

Remarkably, the double-quantum transition has high intensity in the 130 GHz spectrum and its dependence on microwave power, P, does not fit the theoretically predicted $I \propto P^{3/2}$. This result points to a long-standing unresolved question as to the physical nature of double-quantum EPR transitions from coordination complexes; future hf-EPR relaxation studies are expected to elaborate on the subject. In a subsequent study $Ni(NH_4)_2(SO_4)_2$ was measured [24,43]. This is a lower symmetry Ni(II) center which has $g_{iso} = 2.2$, $D = 2.24$ cm^{-1}, $E = 0.38$ cm^{-1}. The material is completely EPR silent in X-band. The 35 GHz spectrum has only two broad features from incomplete $\Delta m = 1$ transitions. At 130 GHz the complete spectrum is observed and is strongly dominated by the relatively isotropic half-field, $\Delta m = 2$ transition where the $\Delta m = 1$ transitions are spread out from rhombicity ($E = 0$).

Copper Cu(II) ($3d^9$, $S = 1/2$, $I = 3/2$) has been the subject of a V-band EPR study on a set of pure, undiluted polycrystalline compounds of the type Cu(amino acid)$_2$ [44]. As with the Cr(V) compounds, mentioned above, at X-band usually only a single, broad line is observed due to exchange broadening. Raising the frequency to 65 GHz is not enough to obtain complete resolution, however, resolved **g**-matrices are observed. In some other complexes, e.g. Cu–tetraphenylporphyrin, exchange broadening is reduced due to the increased size of the ligand, and the spectrum is already partially resolved in X-band. For these systems raising the frequency to V-band affords a simplified spectrum through disentanglement of the electronic Zeeman interaction from the Cu hyperfine interaction; this is equivalent to the V(IV) case described earlier.

Second and third row transition ion complexes have thus far not been studied with hf-EPR.

4.2. Clusters of d-ions

Molecular clusters of transition ions are interesting as possible new materials and they are studied as model systems for, e.g. resonant magnetization tunneling. These clusters frequently have unusual paramagnetism from a very high system spin, which makes them interesting subjects for hf-EPR [45,46]. Only powder samples have been studied thus far. Ionic metal clusters are also abundantly present in biological systems but these have so far not been tackled with hf-EPR.

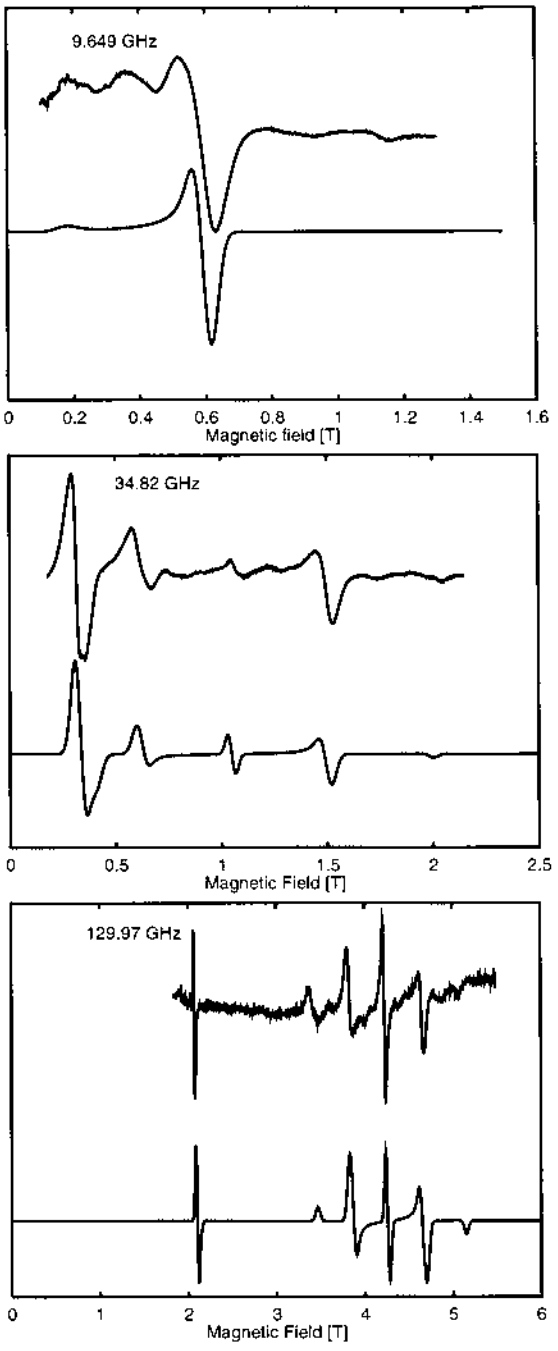

Fig. 2. X-, Q-, and D-band spectra and simulations of the $S = 1$ system Ni(II) (4%) in $[Zn(en)_3](NO_3)_2$. The complete and fully resolved triplet spectrum is only observed at high frequency. Note the dominant contributions from the half-field transition at 2.1 T and the double-quantum transition at 4.3 T in the D-band spectrum. Taken from Ref. [42]; reproduced by permission of Academic Press.

The Fe_8^{3+} cluster $Fe_8O_2(OH)_{12}(tacn)_6^{8+}$ has been studied with 245 GHz EPR [47]. The essentially flat cluster has an $S = 10$ ground state with $g_{\|} = 2.04$, $g_{\perp} = 2.00$, $D = -0.191\ cm^{-1}$, $E = 0.032\ cm^{-1}$. The low-temperature relaxation of the magnetization is in between that for ferromagnets and isolated molecules and points to an Orbach relaxation mechanism.

The Mn_4 cluster Mn(IV)Mn_3(III) in the trigonal pyramidal complex $[Mn_4O_3Cl(O_2CCH_3)_3(dbm)_3]$ (dbm = dibenzoylmethane) has been studied with hf-EPR [48]. The system is a single molecule magnet with $S = 9/2$ ground state. The axial zero-field splitting is $D = -0.53\ cm^{-1}$ and there is also a finite quartic term.

The Mn_{12} cluster $[Mn_{12}O_{12}(CH_3COO)_{16}(H_2O)_4]\cdot 2CH_3COOH\cdot 4H_2O$ has been measured up to $\nu = 525$ GHz and $B = 25$ T [49]. The cluster behaves as a single nanomagnet with an $S = 10$ ground state. The zero-field splitting $D = -0.46\ cm^{-1}$, and S^4 terms are also important.

The Cu_3^{2+} cluster bis(μ-benzoato-*O*,*O′*)-bis(benzoato-*O*)-bis[μ-(2-diethylamino)-ethanolato-*O*,*N*]bis(methanol)tricopper(II) (CuEtBz · MeOH) has been studied in X-band and at 245 GHz [50]. Single crystal X-band EPR at 4.2 K determined the ground state to be $S = 3/2$ with effective g-values for the $m_S = 1/2$ doublet $g = 4.7$, 4.0, 2.1. The powder exhibited a peak at $g' = 4.3$ moving to $g' = 2.6$ at r.t. The 245 GHz spectra did not show this shift as a function of temperature and this observation was instrumental for the conclusion that the shift in X-band was due to thermal population of different, unresolved, levels.

The Cu_8^{2+} cluster $Cu_8(O_2)(O_2CCH_3)_4(chp)_8$, where chp = 6-chloro-2-pyridinate, has been measured in frozen solution and as powder in X-, Q-, and W-band [51]. The ground state is $S = 1$ with $D = 0.328$, $E = 0$, $g_{\|} = 2.35$, $g_{\perp} = 2.066$. Small single crystals could only be studied in W-band due to the increased filling factor (see also Cu(II)azurin, below).

4.3. Lanthanides

Gadolinium Gd(III) ($4f^7$, $J = 7/2$) complexes in aqueous solution are of medical relevance as contrasting agents in MRI through their influence on water proton relaxation rate. The effect is directly related to the electronic T_1 of the $S = 7/2$ spin at physiological temperatures, therefore, the determination of T_1 is an extremely useful parameter in research on synthesis of Gd(III) complexes as new contrasting agents. Hydrated Gd(III) ion, Gd(III)dtpa, and similar complexes in water all give a single isotropic line in r.t. EPR, whose width is due to the modulation of the zero-field splitting reflecting dynamic distortion of the complexes. From 3 to 140 GHz (S- to D-band) the width of this line in field units decreases with increasing frequency. Furthermore, in D-band EPR the line width, Γ, varies with the temperature of the aqueous solution, and a method has been developed to estimate T_1 from the Γ versus T plot [5,6]. From this we can conclude that aqueous solution hf-EPR, using single-mode resonators, is not only practical but is also more than an academic exercise.

Erbium Er(III) ($4f^{11}$, $J = 15/2$) has been caged in a fullerene, $Er@C_{82}$, and its EPR has been studied at 80 GHz [25]. The spectrum shows broad features from an anisotropic effective **g**-matrix and extends over a wide field range, ca. 0–10 T. The

spectrum was fitted with effective g-values, $g_{\|} = 4$ and $g_{\perp} = 8.8$. It was detected with a spectrometer built around a millimeter vector network analyzer using a heterodyne detection scheme without field modulation. The resonator was of the oversized type. The interest of this study is in the description of a novel spectrum and, furthermore, as an illustration of an unconventional and promising way of hf-EPR spectroscopy on randomly oriented samples.

Other metallo-fullerenes, $M@C_{82}$ (M = Sc, Y, La) have been studied with the Bruker pulsed W-band spectrometer to obtain increased **g**-matrix resolution [52].

Thulium Tm(III) ($4f^{12}$, $J = 6$) in ethylsulfate, ES, crystals have been studied with $\nu = 1$–1.6 THz and $B < 10.5$ T [53]. EPR transitions between the singlet ground state and the first excited doublet were observed for the first time (see also [54]). The zero-field splitting is 28.9 cm^{-1} for LaES:Tm(III) and 31.3 cm^{-1} for the pure TmES. The study of these integer-spin systems with large splittings obviously required hf-EPR with fir sources.

4.4. Defect centers

Although defect centers are perhaps not a subject of coordination chemistry per se, they are mentioned here because published work illustrates specific applications of hf-EPR that may be of potential interest also for studies on molecular complexes.

Shin et al. studied the system $Cs^+(18\text{-crown-}6)_2X^-$ in which $X^- = e^-$, Na^-, or Cs^- [55]. These systems contain defect electrons at an anionic site whose chemical nature is uncertain. Increasing the EPR frequency from X-band to 250 GHz results in a significantly increased **g**-matrix resolution. Analysis by simulation indicates the presence of two different trapped electron centers. In addition to illustrating increased resolution at higher frequency this study is of general interest in describing the loading of thermally unstable samples into hf-EPR apparatus.

The EPR spectrum of the intrinsic shallow electron center in AgCl consists of an isotropic, structureless line at $g = 1.878$. Again, the chemical nature of the center is not known with certainty; it is likely to reside on an Ag^+ lattice position. Pulsed ENDOR at 95 GHz produces very rich $^{107;\ 109}Ag$ and $^{35;\ 37}Cl$ spectra [56] (see also [57–62]). Straightforward simulation of these spectra indicates the center to be very shallow indeed, as interaction with Ag up to the 68th silver shell and with Cl up to the 49th chlorine shell is retraceable. The study illustrates the potential strength of special forms of hf-EPR in producing highly resolved superhyperfine structural information.

4.5. Biological systems

Hf-EPR spectrometers have lower concentration sensitivity than standard X-band apparatus. Acceptable S/N ratios are more easily obtained with $S = 1/2$ radical signals than with metal ions, due to smaller g-anisotropy and smaller line widths, and hf-EPR publications on biological radicals still outnumber those on metalloproteins. The majority is concerned with bacterial and plant photosynthetic

systems i.e. radicals from reaction centers, quinones, and tyrosine (cf. [63–71]). Other work is concerned with radicals in enzymes, apo-galactose oxidase [72], $Tyr^{\bullet}$ in ribonucleotide reductase [73], or on amino acid model systems [74]. Spin labels [75–77] and spin traps [78] have also been studied.

Hf-EPR on metalloproteins have thus far been limited to systems with high-spin Fe(III), Mn(II) and Cu(II).

Iron Fe(III) high-spin ($3d^5$, $S = 5/2$) has been studied in hemoglobin from 70 to 400 GHz [16]. This very early (1973!) paper by Y. Alpert et al. is undisputably the classic in biological hf-EPR. The high value, $g \approx 6$, of the effective perpendicular g-value from the transition within the $m_S = \pm 1/2$ doublet afforded measurements up to high frequency where only a maximum field of 6 T was available from a supercon. The intrinsically low S/N ratio of the transmission experiment was compensated by working at low T, 1.5 K, high concentration, 10 mM, and by using high output-power backward-wave oscillators as microwave sources. The effective g-value started to shift significantly from its low-frequency limiting value above ca. 100 GHz and this allowed for a relatively accurate determination of the zero-field splitting, $D = 10.7\ cm^{-1}$. Unexpectedly, it was discovered that the inhomogeneous line width increased approximately proportional with the square of the frequency, $\Gamma \propto \nu^2$, i.e. a decreased spectral resolution with increased frequency. Follow-up studies into this intriguing phenomenon were announces [ibidem], but not carried out due to the sad early decease of the first author. It was later suggested that this unusual broadening is the result of a normal distribution in the axial zero field splitting value, D-strain, due to the same protein conformational distribution responsible for broadening by g-strain [79]. But it was only recently, 25 years later,

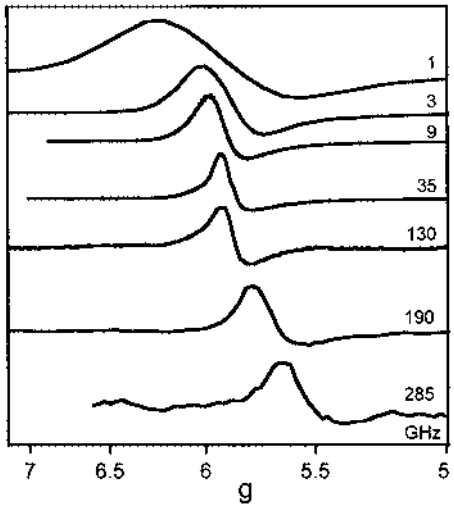

Fig. 3. Normalized multi-frequency EPR spectra of the $g_{eff} \approx 6$ line from high-spin Fe(III) in metmyoglobin (5 mM). The normalized line width first decreases with increasing frequency, but beyond 35 GHz the line width increases again. The effective g-value is constant up to 35 GHz and then decreases towards $g_{real} = 2$. Taken from Ref. [80]; reproduced by permission of the Royal Society of Chemistry.

that the experiment of Alpert et al. was repeated on myoglobin, and the broadening mechanism was indeed identified as D-strain on the basis of powder pattern simulations [80].

This latter study was carried out over the 1–285 GHz frequency range (see Fig. 3) and identified three frequency windows in which different broadening mechanisms were dominant: unresolved superhyperfine broadening at low ν (≤ 3 GHz), g-strain at intermediate ν, and D-strain at high ν (> 100 GHz). The study points out that resolution does not necessarily increase, or even remain constant, with increasing frequency, and that an educated choice of the optimal hf-EPR frequency very much depends on what interaction or distribution of interaction one is interested in.

Two simulation studies have appeared describing predicted EPR powder patterns at high frequency, based on estimated D-values, for non-heme high-spin Fe(III) in rubredoxin [81] and lipoxygenase [82] and for the $S = 3/2$ MoFe cofactor of nitrogenase [81]. These exercises may be useful in predicting future experiments specifically frequency-dependent shifts of effective g-values and appearance of hf transitions that are impossible at X-band. It should be noted, however, that hf-EPR spectrometers that have the concentration sensitivity to actually measure these signals are available. Indeed, hf-EPR (> 95 GHz) data have very recently been obtained for non-heme high-spin Fe(III) in phenylalanine hydroxylase [83] and in rubredoxin [84].

Manganese Mn(II) ($3d^5$, $S = 5/2$, $I = 5/2$) occurs in two mononuclear forms in biology from the point of view of the EPR spectroscopist: the large-D form and the small-D form. In the active site of enzymes (e.g. in the Mn superoxide dismutase) $D \gg 0.3\ cm^{-1}$. In combination with the resolved Mn hyperfine pattern this typically results in complex, highly anisotropic X-band spectra. Hf-EPR has not yet been reported on these systems nor on the X-band EPR silent associated Mn(III) form ($S = 2$). Hydrated Mn(II) ion has $D \ll 0.3\ cm^{-1}$ and gives the well known isotropic six-line pattern around $g = 2.0$. In X-band the lines are broadened through unresolved (or poorly resolved) higher-order contributions in hyperfine and zero-field interactions. At higher frequencies the spectrum sharpens as the higher-order contributions loose significance (cf. the study on d^5 Fe in zeolites cited earlier). This type of Mn(II) can replace Mg(II) in ternary complexes with nucleotides and proteins. This form of Mn(II) in the GTPase protein p21ras has been studied with 95 GHz EPR [85]. ^{31}P-NMR shows that this molecular-switch protein is locked in a mixture of two conformations when reacted with a GTP analogue, however, the heterogeneity is not reflected in the coordination of the Mn(II) because it is not seen in the sharp hf-EPR. In a 140 GHz study on p21ras, by another group, the sharpening effect has been used to facilitate the measurement of ^{17}O hyperfine interactions from water ligands to the Mn(II) and to determine the number of coordinating H_2O ligands [86].

Copper Cu(II) ($3d^9$, $S = 1/2$, $I = 3/2$) in the small electron-tranferring protein azurin has been studied extensively in W-band by Coremans et al. [87–90] and this work is an instructive illustration on several counts of the usefulness of hf-EPR on

metalloproteins. The 3D structure has been determined with X-ray crystallography, however, the crystals are too small to give workable signal amplitudes in single-crystal EPR at X-band. Placing them in a single-mode resonator of ten-fold smaller fundamental wavelength (i.e. W-band, 95 GHz) results in a 10^3 times better filling factor and, therefore, in a highly increased absolute sensitivity. Although the unit cell contains 16 azurin molecules, it proved possible to determine a complete set of angular dependent spectra, and from these the orientation of the $\boldsymbol{g}^2$ tensor in the molecular axis system was determined. The W-band bridge used was of the pulsed type, which would have been a disadvantage for the determination of powder spectra, but this was turned into an advantage because it allowed for $^{14}N/^{15}N$ ESEEM spectroscopy on the coordinating N from histidine (in X-band ESEEM the remote N is measured).

5. Outlook

Over the past decade high-frequency EPR spectroscopy of transition ions has steadily evolved from an esoteric oddity to a reasonably practical, sophisticated research tool. This development has not ended. Major breakthroughs in hardware are expected to occur in the next few years in pulsed hf-EPR/ENDOR in the 200–400 GHz frequency range and, on a somewhat longer time scale, in cw hf-EPR using very wide range static fields.

Although comparison with conventional X-band EPR spectroscopy in general is still unfavorable in terms of concentration sensitivity and ease of operation, the performance of—not so very—high frequency machines, especially the W-band spectrometers, is approaching the X-band standard. Matters become worse (and worse) at higher (and higher) frequencies, but comprehensive research programs directed at sensitivity improvement are underway in several laboratories.

At this time the number of published studies in transition ion hf-EPR is limited to a few dozen (one dozen in metalloprotein hf-EPR). A vast area remains to be explored. Second and third row d-ion complexes are untouched, and so are some of the 3d metals, e.g. cobalt. Many of the integer-spin systems thus far known to be 'EPR silent' await their first trial experiments. This is particularly true in bioinorganic chemistry: Mn(III), Fe(II), Co(I), Ni(II), Mo(IV), W(IV) are all catalytically competent redox states of important enzymes. Furthermore, no hf-EPR studies have been published on biological metal clusters, although the ubiquitous Fe/S clusters frequently exhibit complex paramagnetism, e.g. with very high integer system spin particularly suitable for research in this field. Taking one step further, one could envision very hf-EPR being applied to the characterization not of the ground state spin manifold of these systems, but rather of the whole spin ladder of manifolds whose zero-field splittings from strong exchange interactions are of the order of tens of wavenumbers.

The interested (bio)coordination chemist should now enter the field armed with the balanced insight that hf-EPR opens up fundamentally new possibilities, but that at the same time concentration sensitivity is a key matter of concern (and a

monotonically decreasing function of frequency!). Also, as usual in modern spectroscopy, the word 'high' is not only suggestive of the putative importance and quality of obtainable results, but also of the purchase price of the required hardware. Thus, hf-EPR spectrometers are not homogeneously distributed over the research community and, furthermore, the presently available machines form an inhomogeneous set in terms of sensitivity and possibilities (e.g. with respect to loading of unstable samples). Under these circumstances it will pay off to put more than just a bit of preparative effort in trying to match sample properties, spectrometer specifications, and expected information. This review was written to assist the chemist in that effort.

Acknowledgements

The development of biological hf-EPR spectroscopy in Nijmegen is supported by the European Commission's TMR Access to Large Scale Facilities Programme through grant 'Umbella' ERBFMGECT-950008.

References

[1] D.M.S. Bagguley, J.H.E. Griffiths, Nature 160 (1947) 532.
[2] Brochure EPR/B1200/9707/ha, High-frequency EPR, Bruker Analytik GMBH, Germany.
[3] B. Cage, A.K. Hassan, L. Pardi, J. Krzystek, L.-C. Brunel, N.S. Dalal, J. Magn. Reson. 124 (1997) 495.
[4] D.P. Goldberg, J. Telser, J. Krzystek, A.G. Montalban, L.-C. Brunel, A.G.M. Barrett, B.M. Hoffman, J. Am. Chem. Soc. 119 (1997) 8722.
[5] D.H. Powell, A.E. Merbach, G. González, E. Brücher, K. Micskei, M.F. Ottaviani, K. Köhler, A. von Zelewsky, O.Ya. Grindberg, Y.S. Lebedev, Helv. Chim. Acta 76 (1993) 2129.
[6] D.H. Powell, O.M. Ní Dhubhghaill, D. Pubanz, L. Helm, Y.S. Lebedev, W. Schlaepfer, A.E. Merbach, J. Am. Chem. Soc. 118 (1996) 9333.
[7] W.R. Hagen, in: A.J. Hoff (Ed.), Advanced EPR: Applications in Biology and Biochemistry, Elsevier, Amsterdam, 1989, p. 785.
[8] W.R. Hagen, Adv. Inorg. Chem. 38 (1992) 165.
[9] C.P. Poole, Jr., Electron Spin Resonance, 2nd ed., slightly corrected republication, Dover, Mineola, NY, 1996, Ch. 3 and 7.
[10] P. Goy, M. Gross, J. Raimond, in: M. Siegrist, M. Tran, T. Tran (Eds.), Proceedings of the 15th International Conference on IR and mm Waves Orlando, FL, USA, 1990, SPIE Proc. 1514 (1991) 172
[11] P. Goy, J. Raimond, M. Gross, in: M. Siegrist, M. Tran, T. Tran (Eds.), Proc. 16th Int. Conf. IR and mm Waves, Lausanne, Switzerland, 1991, SPIE Proc. 1576 (1991) 354.
[12] F. Muller, M.A. Hopkins, N. Coron, M. Grynberg, L.C. Brunel, G. Martinez, Rev. Sci. Instrum. 60 (1989) 3681.
[13] C. Kutter, H.P. Moll, J. van Tol, H. Zuckermann, P. Wyder, Infrared Phys. Technol. 36 (1995) 245.
[14] L. Paschedag, J. van Tol, P. Wyder, Rev. Sci. Instrum. 66 (1995) 5098.
[15] A. Bertolini, G. Carelli, C.A. Massa, A. Moretti, F. Strumia, M.X. Qiu, U. Mundlein, IEEE J. Quant. Electr. 34 (1998) 238.
[16] Y. Alpert, Y. Couder, J. Tuchendler, H. Thomé, Biochim. Biophys. Acta 322 (1973) 34.

[17] L.C. Becerra, G.J. Gerfen, B.F. Bellew, J.A. Bryant, D.A. Hall, S.J. Inati, R.T. Weber, S. Un, T.F. Prisner, A.E. Mc Dermott, K.W. Fishbein, K.E. Kreischer, R.J. Temkin, D.J. Singel, R.G. Griffin, J. Magn. Reson. A 117 (1995) 28.
[18] L.-C. Brunel, Appl. Magn. Reson. 3 (1992) 83.
[19] (a) G.M. Smith, J.C.G. Lesurf, R.H. Mitchell, P.C. Riedi, in: IEEE Trans. Microwave Theor. Technol. Symp. Proc., Orlando, FL, USA, 1995, p. 1677. (b) G.M. Smith, J.C.G. Lesurf, R.H. Mitchell, P.C. Riedi, Rev. Sci. Instrum. 69 (1998) 3924.
[20] W.T. Silfvast, Laser Fundamentals, Cambridge University Press, Cambridge, 1996, Ch. 11.
[21] T. Matsui, K. Araki, M. Kiyokawa, IEEE Trans. Microw. Theor. Technol. 41 (1993) 1710.
[22] O.Ya Grinberg, A.A. Dubinskii, Ya.S. Lebedev, et al., Dokl. Phys. Chem. 230 (1976) 923.
[23] O.Ya. Grinberg, A.A. Dubinskii, Ya.S. Lebedev, Russ. Chem. Rev. 52 (1983) 850.
[24] E.J. Reijerse, P.J. van Dam, A.A.K. Klaasen, W.R. Hagen, P.J.M. van Bentum, G.M. Smith, Appl. Magn. Reson. 14 (1998) 153.
[25] M.E.J. Boonman, Millimeter Wave Spectroscopy in High Magnetic Fields, Ph.D. Thesis, University of Nijmegen, The Netherlands, 1998.
[26] I. Amity, Rev. Sci. Instrum. 41 (1970) 1492.
[27] E. Haindl, K. Möbius, Z. Naturforsch. 40a (1985) 169.
[28] U. Harbarth, J. Kowalski, R. Neumann, S. Noehte, K. Scheffzek, G. zu Pulitz, J. Phys. E 20 (1987) 409.
[29] W.B. Lynch, K.A. Earle, J.H. Freed, Rev. Sci. Instrum. 59 (1988) 1345.
[30] J.P. Barnes, J.H. Freed, Rev. Sci. Instrum. 68 (1997) 2838.
[31] A. Colligiani, I. Longo, M. Martinelli, L. Pardi, Appl. Magn. Reson. 6 (1994) 217.
[32] G. Annino, M. Cassettari, I. Longo, M. Martinelli, Chem. Phys. Lett. 281 (1997) 306.
[33] T.F. Prisner, M. Rohrer, K. Möbius, Appl. Magn. Reson. 7 (1994) 167.
[34] J. Krzystek, A. Sienkiewicz, L. Pardi, L.C. Brunel, J. Magn. Reson. 125 (1997) 207.
[35] S. Un, J. Bryant, R.G. Griffin, J. Magn. Reson. A 101 (1993) 92.
[36] F. Herlach, J.A.A.J. Perenboom, Physica B 211 (1995) 1.
[37] P.J. van Dam, E.J. Reijerse, A.A.K. Klaasen, M.E.J. Boonman, P.J.M. van Bentum, J.A.A.J. Perenboom, W.R. Hagen, in: P. Collery, J. Corbella, J.L. Domingo, J.-C. Etienne, J.M. Llobet (Eds.), Metal Ions in Biology and Medicine, vol. 4, John Libbey Eurotext, Paris, 1996, p. 27.
[38] M.E.J. Boonman, W. Mac, A. Twardowski, A. Wittlin, P.J.M. van Bentum, J.C. Maan, M. Demianiuk, Phys. Rev. B (submitted).
[39] G. Feher, P.L. Richards, in: A. Ehrenberg, B.G. Malmström, T. Vänngård (Eds.), Magnetic Resonance in Biological Systems, Pergamon Press, Oxford, 1067, p. 141.
[40] G.C. Brackett, P.L. Richards, W.S. Caughley, J. Chem. Phys. 54 (1971) 4383.
[41] D. Goldfarb, K.G. Strohmaier, D.E.W. Vaughan, H. Thomann, O.G. Poluektov, J. Schmidt, J. Am. Chem. Soc. 118 (1996) 4665.
[42] P.J. van Dam, A.A.K. Klaassen, E.J. Reijerse, W.R. Hagen, J. Magn. Reson. 130 (1998) 140.
[43] P.J. van Dam, Multi-Frequency EPR Studies on Biological Systems, Ph.D. Thesis, University of Nijmegen, Germany, 1998.
[44] D. Zhou, R.W. Kreilick, J. Magn. Reson. A 108 (1994) 93.
[45] A.L. Barra, A. Caneschi, D. Gatteschi, R. Sessoli, J. Am. Chem. Soc. 117 (1995) 8855.
[46] A. Caneschi, D. Gatteschi, R. Sessoli, J. Chem. Soc. Dalton Trans. (1997) 3963.
[47] A.L. Barra, P. Debrunner, D. Gatteschi, C.E. Schulz, R. Sessoli, Europhys. Lett. 35 (1996) 133.
[48] S.M.J. Aubin, N.R. Dilley, L. Pardi, J. Krzystek, M.W. Wemple, L.-C. Brunel, M.B. Maple, G. Christou, D.N. Hendrickson, J. Am. Chem. Soc. 120 (1998) 4991.
[49] A.L. Barra, D. Gatteschi, R. Sessoli, Phys. Rev. B 56 (1997) 8192.
[50] P. Fleuschhauer, S. Gehring, C. Saal, W. Haase, Z. Tomkowicz, C. Zanchini, D. Gattaschi, D. Davidov, A.L. Barra, J. Magn. & Magn. Mater. 159 (1996) 166.
[51] H. Käß, E. Goovaerts, A. Bouwen, D. Schoemaker, R.E.P. Winpenny, Bruker Rep. 145 (1998) 36.
[52] S. Knorr, A. Grupp, M. Mehring, U. Kirbach, A. Bartl, L. Dunsch, Bruker Rep. 145 (1998) 40.
[53] H.P. Moll, J. van Tol, P. Wyder, M.S. Tagirov, D.A. Tayurskii, Phys. Rev. Lett. 77 (1996) 3459.
[54] I. de Wolf, P. Janssen, B. Bleaney, Phys. Lett. 108A (1985) 221.
[55] D. Ho Shin, J.L. Dye, D.E. Budil, K.A. Earle, J.H. Freed, J. Phys. Chem. 97 (1993) 1213.
[56] M.T. Bennebroek, O.G. Poluektov, A.J. Zakrzewski, P.G. Baranov, J. Schmidt, Phys. Rev. Lett. 74 (1995) 442.

[57] M.C. Dendeer, O.G. Poluektov, J. Schmidt, P.G. Baranov, Phys. Rev. B 45 (1992) 13061.
[58] M.C.J.M. Donckers, O.G. Poluektov, J. Schmidt, P.G. Baranov, Phys. Rev. B 45 (1992) 13061.
[59] O.G. Poluektov, J. Schmidt, P.G. Baranov, Phys. Rev. B 47 (1993) 13226.
[60] O.G. Poluektov, M.C.J.M. Donckers, P.G. Baranov, J. Schmidt, Phys. Rev. B 47 (1993) 1611.
[61] M.T. Bennebroek, A. Arnold, O.G. Poluektov, P.G. Baranov, J. Schmidt, Phys. Rev. B 54 (1996) 11276.
[62] M.T. Bennebroek, A. Arnold, O.G. Poluektov, P.G. Baranov, J. Schmidt, Phys Rev. B 53 (1996) 15607.
[63] T.F. Prisner, A.E. McDermott, S. Un, J.R. Norris, M.C. Thurnauer, R.G. Griffin, Proc. Natl. Acad. Sci. USA 90 (1993) 9485.
[64] W. Wang, R.L. Belford, R.B. Clarkson, P.H. Davis, J. Forrer, M.J. Nilges, M.D. Timken, T. Walczak, M.C. Thurnauer, J.R. Norris, A.L. Morris, Y. Zhang, Appl. Magn. Reson. 6 (1994) 195.
[65] M. Rohrer, M. Plato, F. MacMillan, Y. Grishin, W. Lubitz, K. Möbius, J. Magn. Reson. A 116 (1995) 59.
[66] M. Rohrer, P. Gast, K. Möbius, T.F. Pristner, Chem. Phys. Lett. 259 (1996) 523.
[67] S. Un, S.X. Tang, B.A. Diner, Biochemistry 35 (1996) 679.
[68] P.J. Bratt, M. Rohrer, J. Krzystek, M.C.W. Evans, L.C. Brunel, A. Angerhofer, J. Phys. Chem. B 101 (1997) 9686.
[69] C.T. Farrar, G.J. Gerfen, R.G. Griffin, D.A. Force, R.D. Britt, J. Phys. Chem. B 101 (1997) 6634.
[70] M. Huber, Photosynth. Res. 52 (1997) 1.
[71] F. MacMillan, J. Hanley, L. van der Weerd, M. Knupling, S. Un, A.W. Rutherford, Biochemistry 36 (1997) 9297.
[72] G.J. Gerfen, B.F. Bellew, R.G. Griffin, D.J. Singel, C.A. Ekberg, J.W. Whittaker, J. Phys. Chem. 100 (1996) 16739.
[73] P.J. van Dam, J.-P. Willems, P.P. Schmidt, S. Pötsch, A.-L. Barra, W.R. Hagen, B.M. Hoffman, K.K. Andersson, A. Gräslund, J. Am. Chem. Soc. 120 (1998) 5080.
[74] M. Brustolon, V. Chis, A.L. Maniero, L.C. Brunel, J. Phys. Chem. A 101 (1997) 4887.
[75] D.E. Budil, K.A. Earle, W.B. Lynch, J.H. Freed, in: A.J. Hoff (Ed.), Advanced EPR: Applications in Biology and Biochemistry, Elsevier, Amsterdam, 1989, p. 307.
[76] Ya.S. Lebedev, in: N.M. Atherton, M.J. Davies, B.C. Gilbert (Eds.), Electron Spin Resonance, vol. 14, Royal Society of Chemistry, Cambridge, 1994, p. 63.
[77] T.I. Smirnova, A.I. Smirnov, R.L. Belford, R.B. Clarkson, J. Am. Chem. Soc. 120 (1998) 5060.
[78] T.I. Smirnova, A.I. Smirnov, R.B. Clarkson, R.L. Belford, Y. Kotake, E.G. Janzen, J. Phys. Chem. B 101 (1997) 3877.
[79] W.R. Hagen, J. Magn. Reson. 44 (1981) 447.
[80] P.J.M. van Kan, E. van der Horst, E.J. Reijerse, P.J.M. van Bentum, W.R. Hagen, J. Chem. Soc. Faraday Trans. I 94 (1998) 2975.
[81] H. Wu, J. Mol. Graph. 14 (1996) 338.
[82] K. Doctor, B. Gaffney, Appl. Magn. Reson. 11 (1996) 425.
[83] P.P. Schmidt, A. Mártinez, A.-L. Barra, T. Flatmark, K.K. Andersson, Fourth Eur. Biol. Inorg. Chem. Conf., Sevilla, Spain, 1998, p. 180.
[84] A.H. Priem, A.A.K. Klaasen, P.J.M. van Kan, E.J. Reijerse, W.R. Hagen, Fourth Eur. Biol. Inorg. Chem. Conf., Sevilla, Spain, 1998, p. 191.
[85] M. Geyer, T. Schweins, C. Herrmann, T. Pristner, A. Wittinghofer, H.R. Kalbitzer, Biochemistry 35 (1996) 10308.
[86] B.F. Bellew, C.J. Halkides, G.J. Gerfen, R.G. Griffin, D.J. Singel, Biochemistry 35 (1996) 12186.
[87] J.W.A. Coremans, O.G. Poluectov, E.J.J. Groenen, G.W. Canters, H. Nar, A. Messerschmidt, J. Am. Chem. Soc. 116 (1994) 3097.
[88] J.W.A. Coremans, M. van Gastel, O.G. Poluektov, E.J.J. Groenen, T. den Blaauwen, G. van Pouderoyen, G.W. Canters, H. Nar, C. Hamman, A. Messerschmidt, Chem. Phys. Lett. 235 (1995) 202.
[89] J.W.A. Coremans, O.G. Poluektov, E.J.J. Groenen, G. Warmerdam, G.W. Canters, H. Nar, A. Messerschmidt, J. Phys. Chem. 100 (1996) 19706.
[90] J.W.A. Coremans, O.G. Poluektov, E.J.J. Groenen, G.W. Canters, H. Nar, A. Messerschmidt, J. Am. Chem. Soc. 118 (1996) 12141.